ÉCOLE POLYTECHNIQUE
FÉDÉRALE DE LAUSANNE

PERMEABLILITY OF CELLULAR ALUMINUM

SANDRA GUARDIA

MSE-390 - MATERIALS PROJECT

PROF. DR. LUDGER WEBER

LABORATORY OF MECHANICAL METALLURGY

LAUSANNE, JUNE 2014

ABSTRACT

Experimental measurements of the permeability of pure aluminum cellular foams, based on the Darcy-Forchheimer regime equation.

The permeability of various castings of aluminum foams was measured applying the equation of the fluid flow through a porous medium, Darcy's law, including the inertial effects term known as Forchheimer term.

A series of compacted salt preforms were produced in order to create the aluminum foams by liquid metal infiltration. The foams were then manufactured and placed in the measurement stand, made from scratch and specially designed to measure both the flow passing through the metal foam and the pressure drop across the foam. The measurements were analysed to obtain the permeability and the friction factor of the foams, and then confronted with existing theory in literature.

The permeability results obtained in this work, despite differing with the model they are compared to, are in agreement with the values measured in other studies for aluminum foams made by replication and with similar parameters. Therefore, the results of this work may be used to know the necessary pressure to be applied to a fluid to force it to flow through the aluminum foams.

Moreover, the final properties of the foam depending on the characteristics of the preform they are infiltrated to will be described and explained, so that new aluminum foams may be produced with the desired properties by knowing which conditions has to satisfy the preform. The manufacturing data of this work may be used, therefore, to get a better understanding and improve the processing of the aluminum foams by the replication method.

CONTENT

NOMENCLATURE

- $D_{preform}$ [m] = mean salt preform diameter
- $L_{preform}$ [m] = mean salt length
- $W_{preform}$ [kg] = salt preform weight
- ρ_{NaCl} [kg/m^3]= salt density
- $V_{preform}$ [m^3] = volume of the salt preform
- Preform relative density [%] = proportion of volume occupied by the salt in the preform
- D_{foam} [m] = mean aluminum foam diameter
- L [m] = mean aluminum foam length in the flow direction
- W_{foam} [g] = aluminum foam weight
- ρ_{Al} [kg/m^3] = pure aluminum density
- V_{foam} [m^3] = volume of the aluminum foam
- V_f, Foam solid volume fraction or Relative density = proportion of the volume occupied by the metal
- Pore volume fraction or Porosity= proportion of the volume occupied by air
- ∇P [Pa/m] = Pressure gradient through the aluminum foam
- μ_{fluid} [Pa·s] = dynamic viscosity of the fluid flowing through the aluminum foam, in this work air, at atmospheric pressure and ambient temperature
- K [m^2] = Permeability of the aluminum foam
- F [m^{-1}] = Form coefficient, see equation 15 for more information
- ρ_{fluid} [kg/m^3]= density of the fluid flowing through the foam, in this work air, at atmospheric pressure and ambient temperature
- A_{foam} [m^2] = cross sectional area of the aluminum foam, perpendicular to the flow direction
- $\dot{V}$ [m^3/s] = volumetric flow rate, volume of fluid flowing entering the aluminum foam per second
- v_D [m^3/(s· m^2)] = average velocity of the fluid flowing through the aluminum foam or Darcy velocity, computed as the volumetric flow rate divided by the cross sectional area of the aluminum foam
- Re [adimensional] = Reynolds number
- Lc [m] = characteristic length, see equation 9 for more information
- P_0 [Pa] = atmospheric pressure
- v_0 [m/s] = velocity of the fluid outside the sample
- ρ_0 [kg/m^3] = density of the fluid flowing through the foam, in this work air, at atmospheric pressure and ambient temperature, which is the density of the fluid outside the foam
- P [Pa] = pressure at a certain point of the sample
- ΔP [Pa] = pressure difference
- c_I [adimensional] = coefficient for the inertial effects in the Forchheimer regime
- g [m/s^2] = gravity acceleration
- h [m] = height of the water column used in the calibration set-up

- ρ_{water} [kg/m^3] = density of the water at ambient temperature and atmosphere pressure
- D_p [µm] = mean particle size of the particles that form the preform that was infiltrated to obtain the aluminum foam sample
- V_o [%] = preform relative porosity
- $K_{thermal}$ [W/(m·K)]= thermal conductivity of the air at 20ºC; 0.0257 W/(m·K)
- c_p [kJ/(kg·K)] = Specific heat capacity of the air at 20ºC; 1012 J/(kg·K)
- ρ_{air} [kg/m^3] = density of the air at 20ºC; 1.2041 kg/m^3
- v_{gas} [m/s] = gas molecule velocity, which was considered to be 500 m/s
- λ [m] = mean free path of air molecules, which is the average distance the particle travels between collisions with other moving particles
- v_{DCorr} [m/s]= corrected Darcian velocity

1 INTRODUCTION

Cellular aluminum foam is an aluminum metal structure having a substantial volume fraction of distributed internal porosity, which use is increasing in recent times due to its advantageous characteristics and properties. One of these properties, its permeability to flowing fluids, permits the heat transfer between a fluid and the solid. In order to implement this property in actual heat exchanging devices, it is necessary to calculate the necessary power that has to be applied to the fluid in order to make it flow through the aluminum foam, which depends on both its permeability and form coefficient.

The permeability of an aluminum foam is a result of the porosity of the aluminum foam, the connections between its pores and the pore length scale, all of which are dependent on the method employed in the fabrication of the aluminum foam.

The aim of this project is to measure the gas permeability of different aluminum foams, varying the pore volume fraction and size, so as to analyse its effect on the permeability of the foam. It is also an objective to extend general understanding of the aluminum foam manufacturing process, so that by choosing the right parameters used in its fabrication the resulting aluminum foam has the desired properties.

To accomplish this objective, several cellular aluminum samples were manufactured by liquid metal infiltration in salt preforms. The variation of both the porosity and particle size of the salt preforms determined the final structure of the aluminum foams. The metal foams were processed and machined to fit the measurement stand.

An experimental set-up was built and calibrated. In this measurement stand, the chosen gas, air, was forced through the manufactured aluminum foam sample, measuring the flow rate and difference of pressure before and after the sample. All the experimental data was then analysed to obtain the permeability and form coefficient of each sample.

If the correlation between the porosity, the interconnectivity and the size of the pore to the final cellular aluminum permeability is known, it will facilitate the production of heat exchange devices based on the use of aluminum foams, as the necessary power to be applied will be known before actually creating the foam. It is also interesting, especially due to its recently rise in usage, the application of these aluminum foams as electrodes for fuel cells and catalytic reactors.

All the materials and appliances involved in this project, from the salt preforms to the aluminum foams, including the measurement stand, have been created at the EPFL LMM, Laboratory of Mechanical Metallurgy.

2 PREVIOUS WORK

With the purpose of having a deep understanding on the topic before starting the practical work, some publications and previous studies on the subject were consulted.

To begin with, a general overview about the aluminum foams is described in the chapter about porous metals by the authors Russell Goodall and Andreas Mortensen [1]. In this publication are explained the main manufacturing methods employed in the production of open-cell aluminum foams as well as its different pore form and connectivity depending on the manufacturing method employed, the aluminum foam structure and principal characteristics and properties, and the commonly used machining procedures. The physical property of being permeable to fluid flow and the law and parameters governing this phenomena were also clarified by means of this publication.

Moreover, the exact mathematical equations for modelling the fluid flow through a porous medium were analysed in more detail in the publication *Flow in Porous Media,* by Dr. R. W. Zimmerman [2]. The explanation of the terms of the equations employed and the complete description of the units employed for the permeability, as well as some reference values for this, were a few of the sections accessed of this document.

The permeability of aluminum open-pore foams produced by the replication method has been measured previously, by using water or glycerine as a flowing fluid, and varying the pore size and the relative density of the foam [3]. The fact that the fluid flowing through the aluminum foams is in liquid state, more viscous than a fluid in gas state, will make the viscous forces exceed the inertia forces. That results in the flow passing through the foam in its steady state, ruled by the Darcy equation (without the Forchheimer term). Therefore, this present work is a similar study as the one done in [3], but with a different fluid whose properties may lead to the establishment of the Forchheimer regime. Furthermore, the permeability values obtained by this work will be compared to the microstructure-based model for the permeability of the open-pore microcellular proposed in [3], with a view to ascertain if this model is still valid when the Forchheimer regime is reached.

The effect of the diameter of a cylindrical aluminum foam on the velocity profile of the fluid flowing through it was investigated in [4]. From this text it is concluded that for small Darcy numbers, meaning small diameters or high permeability, the velocity profile does not depend on the distance to the boundary of the foam with its confining walls. From this it can be concluded that velocity over most of the cross section of the cylindrical foam will remain constant, so that the average velocity inside the foam can be approximated as the free-stream velocity (volumetric flow over the cross sectional area of the foam). Although this result was obtained by measurements of fluids on the Darcy regime, it will be used in this work even if the Forchheimer regimen is reached. The selection of the size of the diameter of the samples used in this work was based on the results of this work.

The friction factor and its dependence of the Reynolds and Darcy number of the flow, as well as on the viscosity of the fluid was also studied in [3]. These parameters are in turn governed by the porosity and the diameter of the cylindrical porous medium, so they can be chosen to influence important flow characteristics such as the velocity profile or the pressure drop of the fluid passing through the porous medium.

Dukhan and Ali [5] examined the effect of the confining walls and the transverse size (perpendicular to the flow direction, as the diameter) of the metal foam sample on its permeability and form coefficient obtainment by applying the Darcy-Forchmeimmer equation. Both the confining walls and the size of the foam sample have a strong influence on both the velocity field inside the foam and the pressure drop, especially for small confined foam size, so that the flow relations may not be applicable or require modifications in order to account for the pressure drop originated by this effect. Not contemplating this effect may lead to erroneous values of the permeability, and is for this reason that the authors experimentally determined a minimum diameter of the cylindrical confined foam to avoid having pressure drop due to this wall and size effect, and so obtain a truthful pressure drop. This will permit the acquisition constant permeability and form coefficient, and neglecting wall and size effects. In this study the experimental values were obtained by means of open-cell aluminum foams subjected to fully-developed air flow in the Forchheimer regime, as will be done in this present work.

Last, it has also been consulted the experiment done in [14], which is the measurement of the permeability and the form coefficient of metal foam, made by metallization of a polyurethane foam followed by a thermal decomposition of the polyurethane and nickel-chromium as a metal. The fluid used in this publication was also air, and even though the foams tested in this publication and the ones used in this work will have different fluid flow through them due to its different properties (a direct result of its pore structure, which completely depends on the manufacturing method), the experimental procedure and results may serve as a guide for this work.

3 THEORY

In this section is explained the theoretical basis on which this work is based. It begins with the description of the structure of porous metals, followed by the explanation of the phenomenon of the fluid flowing through a porous metal and ending with the measure of its permeability.

3.1 Structure of the microcellular aluminum

The structure of porous metals is generally separated in two parts. One is the structure formed by the metal, which may not have the same microstructure as the dense metal because the internal porosity may have an effect on its development. The other part is the structure formed by the assembly of the interconnected pores, that may vary from 90 to 450 µm for the samples used in this work. The properties of a metal foam are, thus, a direct consequence of these two structures, the latter being the most influential. In particular, the permeability of the metal foam, the property studied in this work, is only dependent of the pore structure [1], which is mainly defined by the pore size, shape and interconnectivity.

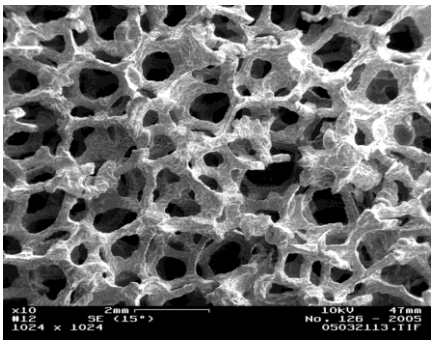

Figure 1: Open cell metal foam in scanning electron microscope

Given the significance of the microstructure of the metal and the internal structure composed of the pores in the properties and characteristics of the porous metal, the acquirement and calculation of the parameters to characterize the metal foam are explained next.

3.1.1 Density

First, it is necessary to differentiate between the relative density of the preform used in the creation of the metal foam and the final density of the latter, which are intrinsically correlated.

The relative density of the salt preform is calculated by dividing its weight by its volume to obtain the density of the preform. This density is then divided by the density of the NaCl, which is the density that it would have if the preform did not have any air gap inside. Thus, it can be known what proportion of the preform is formed by solid particles, which will form the porous structure of the posterior metal foam. The equations used in the calculation of the preform relative density are shown next:

$$V_{preform} = \pi \cdot \frac{D_{preform}^2}{4} \cdot L_{preform} \quad (1)$$

$$Preform\ relative\ density = \frac{W_{preform}}{V_{preform} * \rho_{NaCl}} \cdot 100 \quad (2)$$

The density, or volume fraction solid of the foam is computed in the same manner as the relative density of the preform but using this time the density of aluminum:

$$V_{foam} = \pi \frac{D_{foam}{}^2}{4} \cdot L \quad (3)$$

$$Foam\ solid\ volume\ fraction = \frac{W_{foam}}{V_{foam} \cdot \rho_{Al}} \quad (4)$$

Therefore, the preform porosity (or pore volume fraction) is the unit minus the relative density of the preform in percent, and the foam porosity is as well the unit minus the foam volume fraction for one unit.

$$Porosity = 1 - Foam\ solid\ volume\ fraction \quad (5)$$

Theoretically, the *preform relative density (eq. 2)* and the *foam solid volume fraction (eq. 4)* sum to 1, but it will be seen later that this does not always happen, mostly owing to the possible existence of residual pores or to the presence of remaining salt particles.

3.1.2 Pore size and shape

The pore size of the samples used in this work has not been measured (which could be done by manual or imaging techniques [1]), but considered as being the same as the size of the salt particles that formed the preform. As for the shape of these pores, given the complex shapes of the salt particles, has been assumed as being a sphere of diameter equal to the pore size.

Figure 2: two different pore size aluminum foams made for this work

3.2 Fluid flow through metal foams

The fact that a fluid may pass through a metal foam, allowing the heat and mass transport between them, is the main reason why highly porous metal foams are being looked into [1].

The permeability is defined as a measure of the ability of a porous material to allow fluids pass through it. This property determines in part the necessary excess of pressure that has to be applied to the fluid to make it flow through the metal foam, in a steady-state at a unidirectional average velocity, through a unit of length of the porous medium [1]. It has to be remarked that the permeability is a property that is only defined for a porous medium, and that cannot be considered for a certain point of that porous medium [2].
For the velocities and pore size of the samples analysed in this work, the unidirectional flow through a homogenous isotropic material is ruled by the Dupuit-Forchheimer modification of Darcy's law [1-5]:

$$-\frac{\partial \mathrm{P}}{\partial \mathrm{x}} = \frac{\mu_{fluid}}{\mathrm{K}} \cdot v_D + \rho_{fluid} \cdot \mathrm{F} \cdot v_D^2 \qquad (6)$$

This equation is equal to this equation expressed below:

$$-\nabla P = \left(\frac{\mu_{fluid}}{K} + \rho_{fluid} \cdot F \cdot \|v_D\|\right) \cdot v_D \qquad (7)$$

Where P is the local pressure of the fluid, x is the distance along the direction of the flow, and v_D is the superficial or Darcian fluid velocity, which is computed as follows:

$$v_D = \frac{\dot{V}}{A_{foam}} \qquad (8)$$

Where $\dot{V}$ is the volumetric fluid flow and A_{foam} is the area of the porous medium perpendicular to the fluid flow.

The flow depends on the fluid characteristics, the dynamic viscosity of the fluid μ_{fluid} and its density ρ_{fluid}. The parameters characterising the porous medium are its permeability K and the drag form coefficient F, which represents the obstruction of the internal structure [11]. In this case, the solid, which is the aluminum foam, is assumed to be isotropic, so this parameters are scalars. In the event that the foam was actually anisotropic, as the flow is in one of its principal directions, this fact would not change.

Equation (7) may be split in two terms. The first term corresponds to the Darcy regime, which considers the viscous friction losses experienced by the fluid flowing through the porous material. This losses may be important if the fluid is complying the no-slip condition with the internal porous surface. The second is known as the Forchheimer regime term, and accounts for the significant inertial forces for high fluid velocities. This is linked to the resistance to flow through the foam, owing to the irregular path that the fluid has to follow or to the pore-scale eddies that may be formed within the fluid [1].

The transition from the Darcy to the Forchheimer regime takes place for a certain value of the Reynolds number:

$$Re = \frac{\rho_{fluid} \cdot v_D \cdot L_c}{\mu_{fluid}} \qquad (9)$$

Where the characteristic length L_c, owing to the fact that the fluid is flowing though porous media, may be defined as: the average pore size, the $\sqrt{K}$ or even K·F depending on the publication reviewed. Each of this definitions of L has its own transition Reynolds number that varies with the material of the porous medium as well as with the author.

With respect to this work, as the fluid employed is compressed air, whose dynamic viscosity value is low compared to liquid fluids and that will reach high velocities while passing through the foam; so that inertial forces will dominate and the flow will be governed by the Forchheimer regime [10], depending on the quadratic value of the Darcy velocity.

3.3 Measurement of the permeability

Up to date, there are several publications about the measurement of the permeability of open-pore porous metals [7] (*e.g.* [3-6]). Some of them, as will be done in this work, are conducted using air as the flowing fluid, commonly performing the experimentation at room temperature.

The measurement of the permeability normally follows the same procedure: a fluid is forced to flow through the straight sample of metal foam, completely fulfilling it, and the volume or mass of fluid per second that traversed the sample and the pressure differential across the sample are alternatively either imposed or measured. This depends on the experimental set-up employed; in this work the volumetric flow will be imposed and the difference of pressure between the two ends of the sample will be measured.

The metal foam sample used for the measurements must fulfil a number of requirements for the morphological parameters of the test sample. First, the sample to pore size ratio must be high [10], meaning that the diameter of the foam must be at least 20 times bigger than the mean pore size. To assure that the measured average flow rate is representative of the metal foam, it is necessary to choose the correct dimensions of the sample to avoid the entrance effects and wall effects. Averting this effects is what entails more experimental difficulty.

Entrance and exit effects may be avoided by testing a sufficiently long sample [8] and by taking the pressure measurements immediately before and after the test sample. Moreover, wall effects are produced either because the borders of the sample deform the pores in its proximity or either because the walls alter the flow path of the fluid in their vicinity. It can also be only because there is a gap between the test sample and the

container wall. This effect can artificially vary the rate of flow, resulting in misleading results of the experiment [11]. The use of tightly fitting container walls, enhanced by covering the test sample with a thermo-shrinkable tube, and the use of test samples, completely fulfilled by the fluid in straight-line unidirectional flow, that show at least 20 pores across their diameter will avoid this effect [6].

If the fluid employed for the experimentation is a gas, as it is the air used in this work, its properties (density and viscosity) are pressure-dependent. It is necessary, thus, to account for the difference of the density of the fluid throughout the sample, provoked by the pressure drop inside the foam. This makes the Darcy velocity not to be constant all through the sample, complicating the application of the continuity eq. 6. Furthermore, as the pressure drop generated between the ends of the sample is big compared to the average of the inlet and outlet pressure, the latter cannot be used as an approximation for calculating the properties of air within the sample, considering them to be constant throughout it. Therefore, in this work it is applied a correction factor to account for compressibility effects within the test sample, as has been done also in the publications [4, 10], which is calculated from eq. 6 as follows:

$$v = \frac{P_0}{P} \cdot v_0 \qquad (10) \qquad\qquad \rho = \frac{P}{P_0} \cdot \rho_0 \qquad (11)$$

Which are the relationship between the Darcy velocity and the density at the pressure at a certain point of the sample, P, and at the atmospheric pressure P_0, which is the pressure at the end of the sample. If the values for P are substituted in eq. 6 for their equivalent in terms of v_0 and ρ_0, using eq. 10 and 11, the next equation is obtained:

$$-\frac{\partial \mathrm{P}}{\partial \mathrm{x}} = \frac{P_0}{P} \cdot \left(\frac{\mu_{fluid}}{\mathrm{K}} \cdot v_0 + \rho_{fluid} \cdot \mathrm{F} \cdot v_0^2\right) \qquad (12)$$

If the integral of eq. 12 is done from the beginning of the sample (x=0) to its ending (x=L), the result is the following:

$$-\int_0^L \frac{\partial \mathrm{P}}{\partial \mathrm{x}} \frac{P}{P_0} = \mathrm{L} \cdot \left(\frac{\mu_{fluid}}{\mathrm{K}} \cdot v_0 + \rho_{fluid} \cdot \mathrm{F} \cdot v_0^2\right)$$

$$\frac{2P_0 \Delta P}{2P_0} + \frac{\Delta P^2}{2P_0} = \mathrm{L} \cdot \left(\frac{\mu_{fluid}}{\mathrm{K}} \cdot v_0 + \rho_{fluid} \cdot \mathrm{F} \cdot v_0^2\right)$$

$$\frac{\Delta P}{L} \cdot \left(1 + \frac{\Delta P}{2P_0}\right) = \left(\frac{\mu_{fluid}}{\mathrm{K}} \cdot v_0 + \rho_{fluid} \cdot \mathrm{F} \cdot v_0^2\right) \qquad (13)$$

Where $\left(1 + \frac{\Delta P}{2P_0}\right)$ is the correction factor, which will be applied in the calculation done in this work, and L is the length of the test sample along the flow direction. ΔP is the pressure differential, which divided by L will give the pressure gradient ∇P, as seen in eq. 7.

A more convenient form of eq. 7 including the correction factor, which is basically eq. 13 divided by the Darcy velocity v_D, will be used in this work to find the values of K and F:

$$\frac{\Delta P}{L v_D} \cdot \left(1 + \frac{\Delta P}{2P_0}\right) = \left(\frac{\mu_{fluid}}{\mathrm{K}} + \rho_{fluid} \cdot \mathrm{F} \cdot v_D\right) \qquad (14)$$

The majority of the plots of the measured data, ΔP, divided by the sample length and multiplied by the correction factor, as the left term in eq. 14, versus the Darcian velocity will show a curve with two differentiated parts. The first is a nearly horizontal line, as a result of the application of the Darcy law, that holds for low values of v_D, from which the permeability can be deduced by knowing the value of μ_{fluid}. As v_D increases, the curve will turn into an ascending line whose slope is the product $\rho_{fluid} \cdot \mathrm{F}$, so by knowing the density of the fluid the value of K may also be deduced. This ascendant linear portion of the curve accounts for the establishment of the Forchheimer regime. The transition from the Darcy to the Forchheimer regime is visible, permitting the approximation of the value of the Reynolds number that sets the transition from the viscosity-dominated to the inertial flow regime.

The value of the permeability K can be deduced from this plot by extrapolating to zero v_D. It is necessary to indicate, though, that the data collected for the inertial regime (with high values of Re) will generally not give the same value of K that may be obtained by considering only the data with low Re values, that account for the Darcy regime [11]. In this work, both values of K will be obtained and compared. It is necessary to clarify that there is actually another possible regime in fluid flow through porous metals, known as the turbulent regime, but it is not considered in this work as the fluid velocities reached in this experimentation are too low for this regime to be established [12].

The values of K that have been measured in previous publications range from 10^{-12} to 10^{-6} m^2 [1, 3-6, 8-11]. This difference in the results, of several orders of magnitude, is explained by many factors. The first one is the dependence of both K and F with the average pore diameter, the first varying as the square of it and the second changing linearly with its inverse [1]. Also, the foam solid volume fraction has a strong effect on the value of K.

The parameter F, which is part of Forchheimer term in eq. 12, is adequately predicted as function of the permeability K [1, 5]:

$$F = \frac{c_I}{\sqrt{K}} \qquad (15)$$

Where c_I is a constant coefficient that accounts for the inertial effects in the Forchheimer regime, and which values obtained in previous publications range from 0.03 and 0.11 [1].

3.4 Calculation of the permeability

Despite the numerous of publications on this subject, it has not been obtained yet an empirical correlation of the two principal parameters defining the foam, the average pore size and its relative density, that gives a good prediction of the values of K and F. This is due to the fact that the resistance of highly porous metals to fluid flowing through it is a direct consequence of its pore architecture, so that the predictions of the value of K and F depend on the way the porous metal was produced, what in turn determines its pore structure [1].

For the porous metals used in this work, which are aluminum foams made by the replication process (explained in the next section), the pore space is determined by the structure of the particles that form the preform. It has been developed a relation between the permeability K and the average pore size and the solid and pore volume fraction of the metal foam made with this method [1], which may be used to accurately predict the permeability of the microcellular foams made by replication:

$$K = \frac{(1-V_f)\cdot D_p^2}{4\pi}\left(\frac{V_o-V_f}{3V_o}\right)^{3}/_{2} \qquad (16)$$

Where D_p is the mean particle size of the particles that forms the preform from which the aluminum foam was infiltrated, and V_o is the result of $(1-V_o)=0.64$, which accounts for the volume fraction of the preform before densification.

3.5 Wall effects

The porous material that is traversed by a fluid is almost always confined by a dense solid, a container, which is where the fluid flows until it encounters the porous material. The fluid flow through the porous material may be altered by the presence of this dense solid, and its consequences will take place along the interface of this dense solid with the porous material that it surrounds. This event may occur for many reasons. It can be a consequence of the deformation of the pores close to the external surface of the porous material or of the presence of an air gap between the porous material and the dense solid. It may also be an effect of the machining or the manner in which the porous material has been fixed to the solid. However, its effects are hard to be accounted for, but usually the affected region will be a layer of the size of a few pores, so it can be neglected without distorting the results much depending only if the pore size is very small compared to the dimension of the sample.

The solid dense surrounding the metal foam also affects the flow through it because of the no-slip condition, which imposes a zero velocity of the fluid in contact with the dense solid surface. The flow region adjacent in which this viscous effects and so the velocity gradient (ranging from zero on the interface of the solid to the Darcy velocity) is significant is known as the boundary layer. This effect is not contemplated in the Darcy-

Forchheimer equation (eq. 12), in which an average velocity is used to describe the flow through plenty of no-slip surfaces. However, neglecting of this effect does not entail the perturbation of the flow through the metal foams, so that the equation can still be used, even for relatively dense metal foams [1]. Moreover, if the transversal area of the metal foam confined in a cylinder container is big enough, the consequences of the wall and size effects are not relevant [5].

3.6 Klinkenberg effect

The fluid flow through a porous medium is different if the fluid is a gas or a liquid, since the gas is highly compressible and also because of the Klinkenberg effect. Klinkenberg demonstrated that the permeability of a porous medium to a gas flowing through it is approximately a linear function of the inverse of the pressure difference applied. This effect may alter the flow through metal foams, especially for low permeability ones. This effect is usually ignored in most the previous calculations of the permeability that have been made before, but it has been experimentally proved that neglecting this effect in foams with low permeability values may lead to false results [13]. The highest permeability value for which it is necessary to contemplate this effect is 10^{-12} m^2 [13], which is one order of magnitude lower than the permeability values that were obtained in this work. It is for this reason that this effect will be not considered in the analysis of the flow through the samples measured.

Moreover, the Klinkenberg effect is relevant in any situation where the mean free path of the gas molecules in porous medium is similar to the pore dimension [2, 13, 15]. In this condition, significant molecular collisions with the pore wall occur more frequently than with other gas molecules, so that the permeability is enhanced by this 'slip flow' [13]. Therefore, this effect is more significant as the pore size of the metal foam is smaller.

To estimate if this effect could be ignored without falsifying the results, the value of the mean free path of the gas molecules in porous media was determined, to see whether it can be compared to the pore size of the samples used in this work. The mean free path of the gas molecules in porous media, λ, will be determined by means of equation of the thermal conductivity of gases:

$$K_{thermal} = \frac{1}{3} \cdot c_p \cdot \rho_{air} \cdot v_{gas} \cdot \lambda \qquad (17)$$

Knowing the values of $K_{thermal}$, c_p, ρ_{air} and v_{gas} at 20ºC, the resulting value of λ turns out to be 0.1265 µm, which is very small even if compared to the minimum of the pore sizes of the preforms used in this work. Therefore, this effect can be excluded for this experimentation, because for the pressure values produced in the measurements this effect is not significant.

4 SAMPLE PROCESSING

The technique employed in the production of the metal foams determines its internal pore structure, which in turn defines its final properties. The aluminum foams used in this work were made by the use of the replication method.

Figure 3: Rubber cylinder filled with the salt particles and covered with the latex

In this work, the samples were made by the procedure of creating the porosity by packing, in particular by a removable phase that acts as a space holder. This method consists in making an assembly of individual elements, which will then be pressurised in order to make them pack and create a structure with gaps that may be filled with the liquid metal, so the pores will take the place of this elements when they are dissolved. With this approach, it is obtained an aluminum foam with the same pore structure that the one made of compacted elements.

The removable phase employed for creating the samples is made of sodium chloride particles of different sizes, so as to obtain different pore sizes in the resulting aluminum foams. The salt particles were sieved and separated in three categories according to its size, the first one ranging from 90 to 125 micrometres, and the rest from 180 to 250 micrometres and from 400 to 450 micrometres respectively. Using salt as a preform material is due to the fact that is a ready available material, non-toxic and easy to handle and to remove, as it completely dissolves in water.

Then, a cylindrical rubber container was filled only with one category of salt particles, and was tapped repeatedly in order to increase the proportion of space filled or packing efficiency. This container was enveloped in a thin sheath of latex so that the particles do not leave the container and to prevent its direct contact with the pressing fluid, i.e. glycerine *(Figure 3)*.

The following step is to apply pressure to the salt particles to increase the contact they make between them, so that they create an interconnected network that will origin the pore interconnectivity of the aluminum foam. In order to compress the structure formed by salt particles, the Cold Isostatic Pressing (CIP) method is applied. This technique consists in depositing the enveloped cylindrical rubber container in a bigger cylindrical container filled with a fluid, in this case glycerine, and apply pressure to the fluid so as to transfer that pressure to the rubber container in all directions. Applying this isostatic pressure will assure a homogenous density of the salt

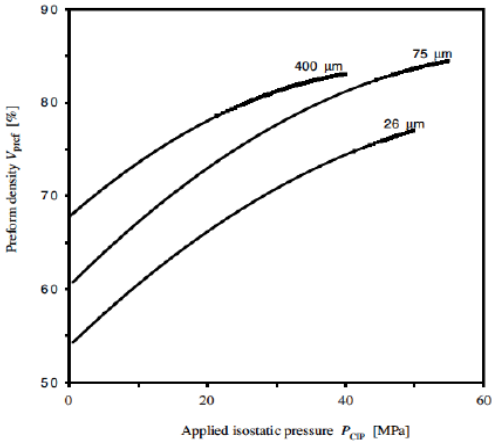

Figure 4: Relationship between the CIP pressures applied and the resulting preform relative density for each salt

preform, being possible to achieve salt preform densities up to 90%. The relationship of the resulting salt preform porosity with the total pressure applied in this technique depends also on the salt particle size, and it was deduced using the graph that indicated the CIP pressure to apply depending on the particle size of the salt preform and the desired porosity *(Figure 4).*

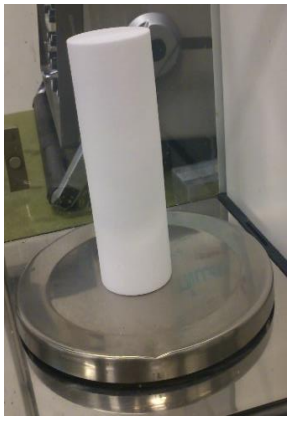

Figure 5: Salt preform being weighted

Then, the salt preforms are extracted from the rubber container cautiously, and consequently weighted and measured in order to calculate its density and corresponding porosity. The resultant salt preform can be seen in *figure 5*.

The relative density of the preform is calculated with eq.1 and eq. 2. Therefore, the preform porosity is the unit minus the relative density in percent, as shown in eq. 5

Once the preforms are made, they are infiltrated with liquid aluminum, so that it fills the gaps of the preform, forming the aluminum foam. This process is called gas-pressure infiltration, and consists in forcing the molten pure aluminum to flow into the salt preform by applying pressure with a gas, in this case argon, in a special oven designed with this purpose. This procedure is possible due to the higher melting point of the salt (801ºC) compared to the melting point of the aluminum (660ºC), so that the salt structure practically does not melt in contact with the liquid aluminum, what would cause the salt particles to blend with the molten aluminum.

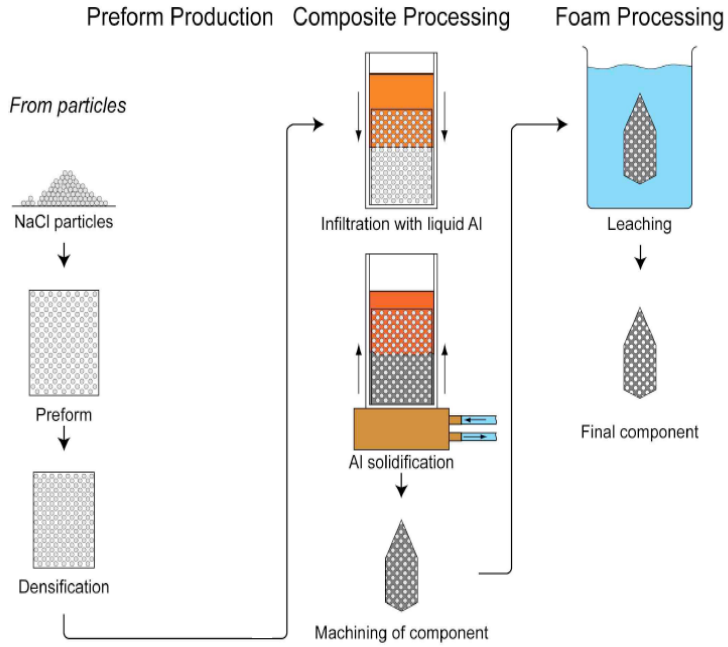

Figure 6: Scheme of the manufacturing of aluminum foams by removable phase or replication method, extracted from [1]

It is very important to carefully control the pressure of the gas during the introduction of the molten aluminum, as it will cause obtaining larger interpore windows. The smaller the salt particle is, the more pressure is needed for the infiltration, and this pressure range applied during this procedure affects the corresponding density of the aluminum foam. This infiltration pressure may also have an effect on the aluminum foam, because for high

infiltration pressures the aluminum might infiltrate even in the small cracks of the salt grains, so increasing the metal volume fraction.

After the aluminum is fully infiltrated at 710ºC and cooled down, the salt preform in its interior is dissolved in water so that it is totally eliminated. The fact that the pores form an interconnected network is essential so that all the salt preform may be removed by this method.
The resulting aluminum foam *(figure 7)* will have a porosity similar to the relative density of the preform from which it is created, meaning that if the preform had a porosity of 20% the aluminum foam will have a porosity of closely 80% and so on.

Figure7: Resulting aluminum foam

Because the aluminum foams are a porous material, most of them have a great workability, and can be machined easily using standard workshop tools. For low density foams, special caution is required during its machining, due to the fact that its lower yield strength may cause the foam to bent and deform while being machined. The machining of the infiltrated preforms becomes easier if the preforms are machined before removing the inner salt structure, because of the greater yield strength of the composite material. This procedure requires the use of tools that cannot be corroded by salt.

The aluminum samples used in this work were machined as cylinders of the same diameter and different lengths.

Once the aluminum foam samples are machined in their final shape, they are cleaned by vibrating the machined foams in a dissolution of ethanol to aid minimizing the amount of residual NaCl and other impurities *(figure 8)*. Then, they are dried by being exposed to pressurised air and disposed in a thermal plate at 200ºC for 20 minutes, to assure its complete drying *(figure 9)*. Once finalized, the samples are let to cool down, and they are then weighted and measured to verify its final porosity and dimensions.

Figures 8 and 9: Leaching and drying of the samples

Below is all the information preforms that were made in this work, as well as its corresponding aluminum foams *(see table 1)*. It includes the particle size range from which the preforms are made, as well as the applied CIP pressure to create them and the resulting

relative density, which gives the information about how porous the preforms are. The infiltrations, which in this work are also called castings, are named from OA to ON in order to distinguish them. For each infiltration, the infiltration pressure that was applied and the relative density of the resulting aluminum foam is also specified.

Some preform numbers are missing (9, 12, 15 and 16) because these preforms were planned to be fabricated but it could not be done at last, and despite this fact the numbering was maintained. Also, the preforms 2,3,4,6 and 11 were never infiltrated, so any sample comes from these preforms. Indeed, the porosity of the preform 11 was so high that the preform fell apart, so that its infiltration could not be done.

The preforms corresponding to the castings OA, OB, OC and OI were already produced, so some of the information related to it its missing. Notwithstanding, as the most important information of an aluminum foam for the purpose of this work is its relative density and particle size, the samples of these castings were also experimented with to determine its permeability.

Preform Number	Particle size [µm]	CIP pressure [MPa]	Preform Relative Density [%]	Casting Name	Infiltration Pressure [bar]	Al Foam Relative Density [%]
1	400-450	25	79,5	OD	5	18,58
2	90-125	33	77,6	-	5	-
3	90-125	40	78,9	-	5	-
4	400-450	12	71,9	-	5	-
5	90-125	40	79,7	OJ	5	29,30
6	400-450	5	64,7	-	5	-
7	400-450	15	73,5	OK	5	27,38
8	90-125	18	67,5	OL	5	39,70
10	180-250	30	74,25	OM	5	22,49
11	180-250	18	-	-	5	-
13	400-450	10	66	OH	5	27,11
14	90-125	25	73,5	ON	5	35,43
17	90-125	25	71,9	OF	5	30,74
18	180-250	20	70,9	OE	5	33,48
19	180-250	40	81,9	OG	5	17,37
-	400-450	50	72	OA	4	13,98
-	400-450	-	-	OB	10	15,58
-	400-450	-	75	OC	10	30,42
-	400-450	-	75	OI	3.3	30,25

Table 1: List of all the salt preforms and infiltrations used in this work to make the samples

5 MEASUREMENTS

As has been previously proven, it is possible to estimate the permeability of a porous medium out of both the pressure drop applied and the rate of volumetric flow of the fluid flowing across it, by applying the eq. 14. It is therefore necessary to obtain the values assumed by the variables of the equation when the phenomenon occurs. To achieve so, a measurement stand had to be created from scratch and tested to verify its functionality and accuracy in data collection.

5.1 Experimental set-up

The measurement stand consists of a pressure meter, a valve, a metal tube split into several parts, one of which with a two orifices to hold the sample, another valve and a flow sensor attached to its open ending. Joined to the two orifices there is the pressure sensor connected to a voltmeter, necessary because the pressure drop measurement device outputs a voltage depending on the pressure difference between two points of the sensor.

The flow meter, a variable area meter, is used primarily for adjusting the amount of flow entering the system, by opening gradually the valve that it has within. It also gives a value of the entering flow, but it is only an approximate value since it is not very accurate and its range is too small for this experiment.

The following component is a valve, used to control the flow entering the metal tube.

Then, a metal tube is formed by metal cylinders joined together. The metal cylinder with the two orifices is located in the middle of this assembly *(figure 10)*. The junction of this metal cylinder with the rest of metal tube is secured by two rubber parts and two nuts, in order to ensure that air does not escape the system. This tube also has a notch located slightly before the second aperture to secure and prevent the sample from being pushed out of the cylinder as a consequence of the pressure differential generated. Once the sample is introduced into this tube and held by the notch, a piece of plastic with small circular holes is also introduced to regulate and homogenize the air flow entering the cylinder and coming across the sample *(figure 11)*. This will prevent the possible formation of eddies if the Forchheimer or the turbulent regime is reached inside the container.

Figure 10: Metal container, with the arrow indicating the flow direction

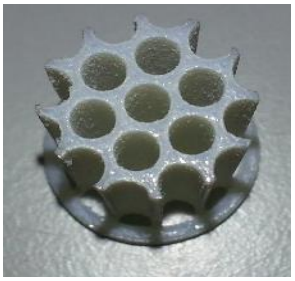

Figure 11: Plastic part inserted in the metal container to guide the flow

After this there is another valve to permit or block the air passing, and next is the ending of the metal tube, with a metal foam to regulate the air leaving the system.

The volumetric flow is measured by the sensor SENSIRION® SFM3000 at the end of the metal tube, which is logged into the computer with its corresponding SENSIRION® data analysis program installed, a program that shows the acquired data in real time and permits its storage in excel files. This sensor is precise enough to give the volumetric flow with tree decimal numbers, measured in standard litres per minute (slm).

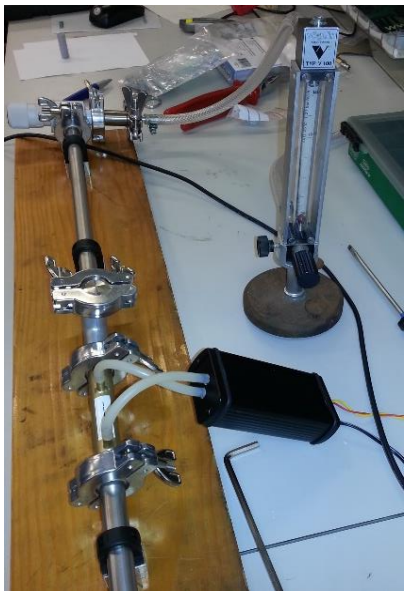

Figure 12: Pressure gauge connected to the metal cylinder, valve and flow meter employed in the experimentation

Two rubber tubes connect the orifices of the metal part holding the sample with the pressure drop measuring device *(figure 12)*. This device converts the pressure difference between its two sensors in a voltage that will be then measured by the voltmeter. The Conrad® free scale semiconductor MPX-2010 DP differential pressure sensor was chosen with this purpose.

Figure 13 shows the internal circuit that had to be connected in a circuit board for the Conrad® MPX-2010 DP differential pressure sensor, where the values of C1, C2, R1, and R2 are 0.1 µF, 1 µF, 240 Ω and 5000 Ω, respectively. V_{IN} is always bigger than 12 V. The purpose of this circuit was to stabilize the supply voltage (V_{IN}, at 10 V), which has some tendency to shift quickly, so as to be able to determine the variation in the voltage due to the measurement of the pressure difference. This is necessary because the Conrad® MPX-2010 DP differential pressure sensor is a ration metric instrument, which gives an outlet voltage depending on the difference of pressure it detects and its inlet voltage.

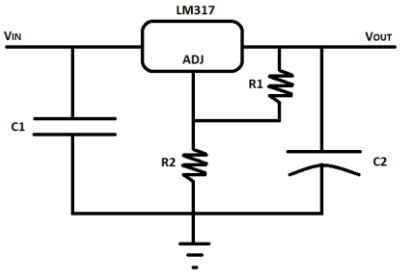

Figure 13: electrical scheme of the voltage stabilizer

Owing to the delicateness of the electronic components that constitute the pressure gauge, the maximum limit for the voltage output at the voltmeter is around 25 mV,

which corresponds to around 100 mbar. If this limit is exceeded, the internal components may break, making the pressure sensor inoperative.

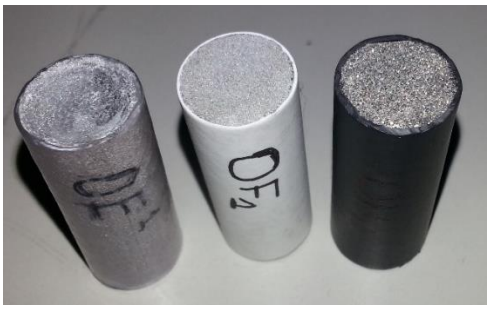

Figure 14: Samples covered with the three types of thermo shrinkable plastic

To avoid obtaining erroneous results, it is necessary to secure the foam in the metal cylinder, and to check that all the air flow passes through the sample and not by its surroundings. To this end, the samples are covered with a shrinkable thermoplastic that conforms to the sample when heated by a dryer. According to the diameter of the sample, that may vary few tenths of a millimetre, and as it has to be very tight inside the containing cylinder, it will be necessary to use a plastic with the lower final thickness after contraction, otherwise the sample will not enter in the metal cylinder. In this work three types of plastic were used; one black, one transparent and one white, sorted from lowest to highest contractibility *(figure 14)*. The excess plastic is then cut by a cutter, so that it only covers the side area of the sample. The plastic cover is coated with a special vacuum grease, which will prevent air from passing between the lateral face of the sample and its confining cylinder. This grease maintains its stability from -40 to 200ºC, and may hold up vacuum pressures below 1333.2 Pa, so it is suitable for this experiment.

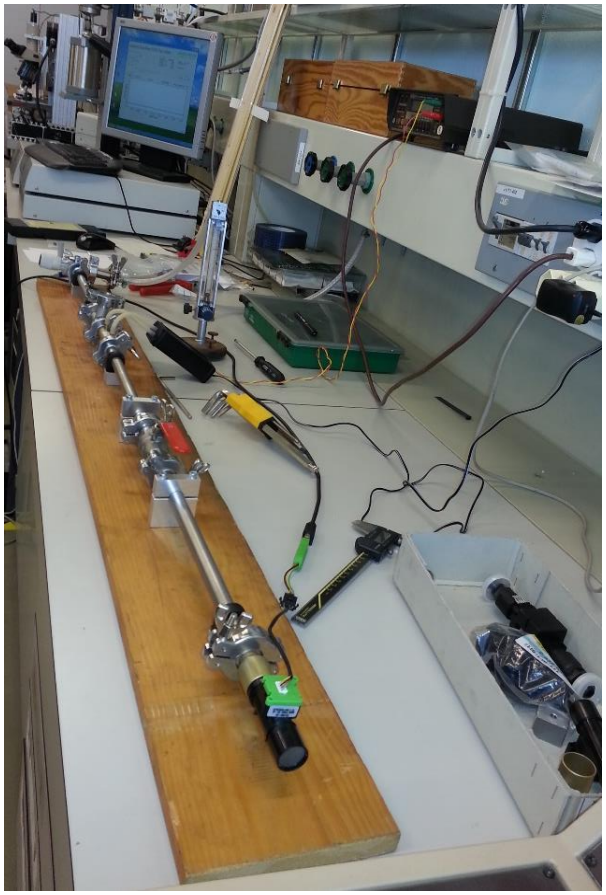

Figure 15: Complete measurement stand

After applying the vacuum grease, the sample is gently introduced into the metal cylinder using a metal bar. This is done so as to avoid applying an excessive pressure to its front are, what may provoke its deformation, closing the pores and so distorting the permeability results. The sample is pushed until it reaches the notch that fixes it to the metal cylinder.

Once the set-up is ready *(figure 15)*, and after inserting the foam sample, the plastic piece is also introduced into the central metal cylinder. Then, the valves are opened to let the compressed air enter the system. By rotating the small wheel in the flow meter the volumetric flow entering the system may be regulated. Thereby, it can be known at all times the air flowing through the sample and

the difference of pressure between its ends, which are the values, required for calculating the permeability of the sample.

5.2 Calibration

Prior to use the pressure drop measuring device, it was indispensable to calibrate it to obtain the relationship of the pressure drop between its endings and the output voltage. To accomplish this, it was necessary to create an additional set *up (figure 16)*. This was formed by a U shaped glass tube with long endings, which is filled with water. One of these endings is left opened, at the atmosphere pressure, and the other is joined to a rubber tube, which is in turn connected to a flow meter attached to the compressed air entrance. One of the sensors of the device is connected to this rubber tube, before its joint with the glass tube, and the other sensor is left unconnected so that it measures the atmosphere pressure. By regulating the flow with the flow meter, the pressure increases, moving the water inside the U shaped tube. The difference of height between the water levels in both endings of the tubes, which was initially zero, will be used to determine the pressure drop:

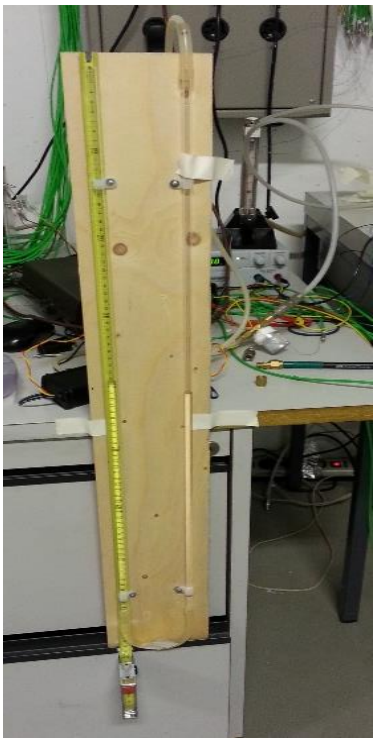

Figure 16: Set-up employed for the pressure gauge calibration

$$\Delta P = g \cdot h \cdot \rho\text{water} \qquad (18)$$

Where h is the height difference, which is twice the distance that has raised the water level in one column by applying the pressure, due to the U-shape of the tube.

Because the other sensor of the device is measuring the atmosphere pressure, there is no need to sum this pressure to the equation.

By doing this, we obtain the voltage outputs of the measurement device, which is connected to a voltmeter, that result from applying a previously known pressure. The relationship of the pressure drop measured by the device and the output voltage is shown next:

$$\text{Output voltage [mV]} = -0,00010157 \cdot \Delta P^2 + 0,24012 \cdot \Delta P - 0,007785 \qquad (19)$$

That has a R^2 value of 0,999976704982982, which means that the adjustment of this equation to the data is acceptable.

The voltage data acquired for this calibration ranges from 0.158 mV to 19.503 mV. Even though the last value is lower than the voltage values that will be obtained in the

measurements (up to 25 mV, which is the limit of the pressure gauge), this function will still be used to convert the measurement results from voltage to pressure, extrapolating it until the 25 mV that are reached in the measurements.

It should be noted that this calibration may not be very accurate, mainly due to the uncertainty in the calibration procedure, for instance in measuring h.

The theoretical basis behind this way of calibrating the device is that the pressure exerted by a column of water is calculated from the height of the water column (see eq. 16), so by knowing the pressure and the resulting response of the device, the dependency between them can be inferred.

5.3 Measurements data

As stated previously, the experiment consists of increasing the air flow through the sample and measuring the corresponding increase in the pressure observed between the extremes of the sample. Hence, during the experiment two values are taken: the air flow passing through the sample and the voltage displayed by the voltmeter, which will be converted into the pressure difference afterwards.

The values of the air flow are taken with the SENSIRION® USB stick sensor located in the extreme of the metal tube that forms the experimental set-up.

The units of the measured flow are standard liters per minute, slm, which is the volumetric flow rate of a gas corrected to the standard conditions of temperature and pressure (0ºC and 1 atmosphere). Even though air density at 0ºC and at 20ºC is different (1.29 g/liter and 1.19 g/liter respectively) as the flow mass is not being calculated, this difference in the temperature condition is not taken into consideration. In order to convert it to the SI units for volumetric rate of flow, m^3/s, the following equality is used:

$$1\ slm = \frac{1\ standard\ litre}{minute} = \frac{1.68875}{P_0} \cdot \frac{Pa \cdot m^3}{s} = \frac{1}{60 \cdot 1000} \cdot \frac{m^3}{s} \qquad (20)$$

The last equality is satisfied if the measurements are taken at atmospheric pressure, and even though this may not be true for the whole experiment, this unit conversion will still be used because the pressure difference within the foam and its consequences are accounted for by using the correction factor expressed in (14).

The data obtained by this sensor is visualized in the computer (*figure 17*), the chosen sampling time is 100 milliseconds and the resolution is 14 bit.
The program also allows to store the data in an excel file, and as the flow value varies continuously within a certain range, this excel data may be used to obtain the mean of these values so as to increase the precision of the measurements. However, this was

only used for some particular data measurements that oscillated too much to determine its value at first glance.

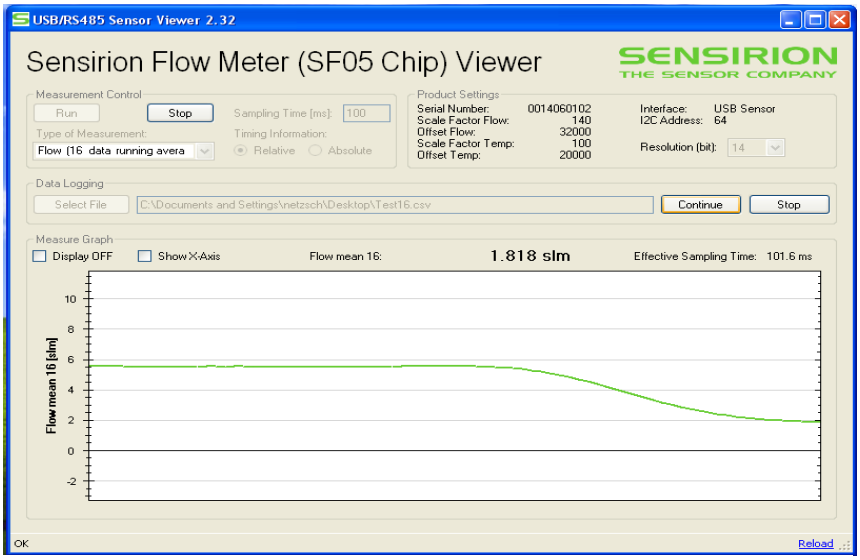

Figure 17: flow measures visualizer

For each air flow value considered, its corresponding voltage in the voltmeter is annotated (*figure 18*). The voltmeter units are mV, which will be converted into Pa by using the inverse of equation (19). The maximum value of air flow measured is the one whose resultant voltage is around 25 mV, so as to respect the pressure gauge limit mentioned before. Depending on the permeability of the sample, the amplitude of the range of the values taken will change, being broader for samples with high permeability values.

The increment between the values measured will be of 0.5 slm from o slm to 5 slm, and an increment of 1 slm from 5 slm to the last value that can be measured. In this way more values are obtained for low flow values, and its consequent low Darcy velocity, that account for the Darcy regime. Once the 25 mV limit has been reached, more measurements are taken in descending order, to get even more data but also to check the validity of the already measured data.

Figure 18: voltage shown on the voltmeter

All the data obtained in this experiments will be stored in excel files, and the necessary calculations for its analysis will as well be done in this files.

6 ANALYSIS

After the completion of all the measurements, it is necessary to analyse the data acquired in order to draw useful conclusions from it. Firstly, the parameters that determine the necessary pressure drop that has to be applied to the fluid to force it to flow through the foam, the permeability K and the drag coefficient F, will be obtained. Thereafter, it will be verified whether these permeabilities obtained from the samples are in agreement with the previously acquired experimental values and the model developed by Despois and Mortensen [1, 3]. Finally, it will be attempted to find a correlation or the relationship between the characteristics of the aluminum foam and its permeability, such that by knowing the first two the latter may be predicted. The effect of the pore size and the porosity of the aluminum foam on its permeability will also be studied separately.

As previously mentioned, the data acquired from the experimentation is the volumetric flow rate traversing the aluminum foam and the output voltage from the differential pressure gauge. This voltage is converted into pressure units by means of the equation obtained from its calibration *(eq. 19)*, the result being the only of the two solutions with physical sense. This pressure value is then converted from mbar to bar units and multiplied by the correction factor *(eq. 13)*. It is then converted to Pa units, in order to have all the values in SI units.

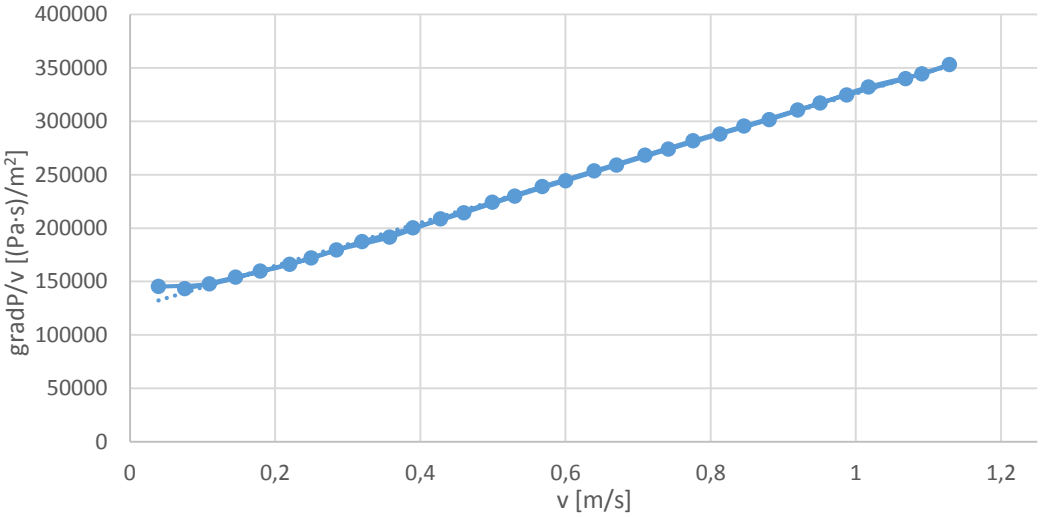

Figure 19: Data plot used for the determination of K and F

The volumetric flow rate is converted from slm to m^3/s *(eq. 20)*, and the Darcian velocity is then calculated *(eq. 8)*. This velocity value would be true if the fluid was traversing a hollow container, but in this case it is flowing through a porous medium, so this value is an approach. If this porous medium is taken into consideration, as the actual cross sectional area is lower than the used in eq. 8, it is possible to approximate the real transversal area by dividing eq. 8 by the porosity of the aluminum foam *(eq. 5)*. The permeabilities using both the Darcian velocity in eq. 8 and the Darcian velocity corrected by the porosity of the aluminum foam will be obtained and compared, so as to confirm if this correction was negligible. Next, the pressure gradient divided by the Darcian velocity is calculated, and

plotted against the Darcy velocity *(figure 19)* so as to be able to determine the parameters K and F from it *(eq. 14)*.

The value obtained by extrapolating to zero Darcian velocity of the second order polynomial that fits the data is μ/K, allowing to determine the permeability K. Also, the slope of this tendency line of the plotted curve accounts for $\rho_{fluid} \cdot F$, so the drag coefficient may also be determined.

It should be also considered that the Darcy regime holds for low Darcian velocities, therefore the first values obtained in the experimentation correspond to this regime, so that the Forchheimer term in eq. 14 may be neglected. Owing to this, the Darcian velocity that marks the transition from the Darcy to the Forchheimer regime will be calculated using eq. 9, but as a characteristic length it will be used the mean pore diameter as was done in [12]. This is because the other characteristic length that may be used in eq. 9 depend on the value of K and F, which are to be determined. All the data that was obtained for lower velocities will then be fitted by a first order tendency line to determine the permeability. The permeability values obtained in this manner will be compared then to the ones obtained if the Forchheimer regime is considered. The other two possible regimes for fluid flow through metal foams, the post-Forchheimer unsteady laminar and the fully turbulence [12], will not be considered in this work, as the Darcian velocities needed for these regimes to be established are too high compared to those that were reached in the experimentation.

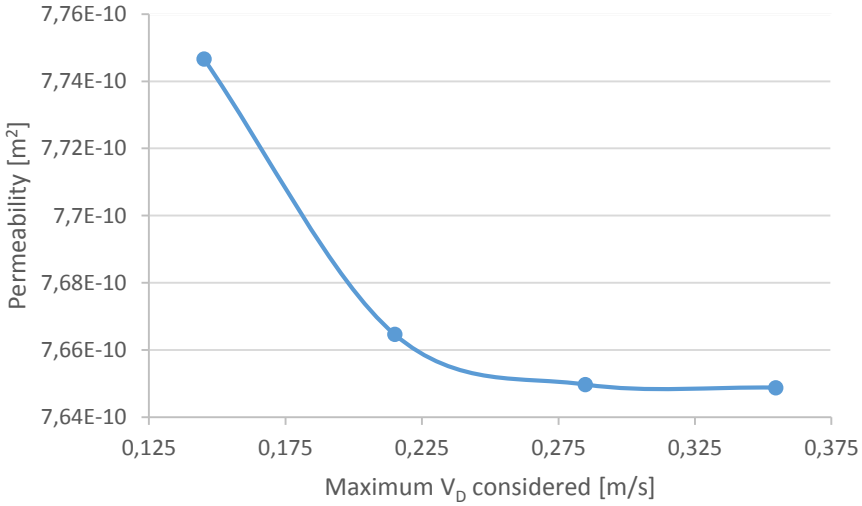

Figure 20: Darcian permeability obtained for different values of the transition Reynolds number considered

The Reynolds number for the transition between the Darcy and the Forchheimer regime for metal foams calculated with the Reynolds number with the pore diameter as a characteristic length is between 1 and 10 [12], and will be considered as 10 for this work. This is because for lower Re numbers, only one or two data measurements may be considered in the Darcy regime, consequently the permeability values obtained for the Darcy regime are less credible. Also, the Darcian permeability value seems to stabilize for bigger transition Reynolds numbers considered *(figure 20)*.

All the parameters used in the equation are in the SI system, so as to obtain the values of K and F in the SI units as well, which are m^2 and m^{-1}, respectively.

6.1 Entrance effect

When the fluid enters the aluminum foam, the pressure drop is affected by the entrance/exit effect, which is due to the transition to the steady flow inside the foam. If the foam is not long enough for the flow to stabilize, the measurements made from it are being distorted by this effect.

With the aim of determining the minimum length of the samples so that this effect does not falsify the results, samples of the castings OA and OB of different lengths were created. Then, the permeabilities of each of these samples were obtained and compared so as to determine the minimum length of the samples that will certify that this entrance effect may be avoided.

The samples of the OA and OB castings have the same pore size (400-450 µm) and similar relative densities. The different values of their permeabilities is, thus, a direct consequence of the infiltration pressure, which was 4 bar and 10 bar respectively. This is the reason why the permeability of the sample OB is lower.

The following table shows the different sizes of the samples used in this analysis, as well as its measured permeability. It can be seen that the permeability for the samples bigger than 20mm in length barely changes, concluding that no significant length effects occur for lengths above that value.

Sample	Length [mm]	Permeability [m^2]
OA1	30,01	8,37456E-10
OA2	20,11	8,94495E-10
OA3	10,06	9,19547E-10
OA4	5,04	7,74782E-10
OB1	40,04	7,02813E-10
OB2	29,98	7,12648E-10
OB3	20,02	7,01259E-10
OB4	10,01	6,63308E-10
OB5	5,01	5,87498E-10

Table 2: samples used in the analysis of the entrance effect

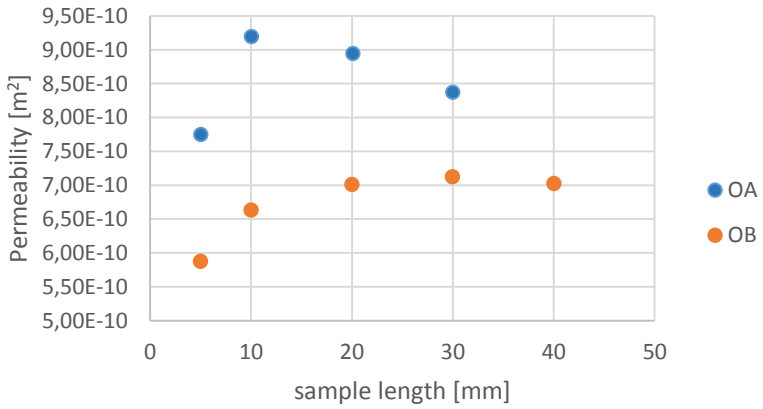

Figure 21: Permeability of the OA and OB castings depending on the sample length

After examining the permeabilities of the samples *(figure 21)*, it was concluded that a length of 30mm would be enough to prevent this effect from affecting the results of the experiment. This is because the value of K seems to become constant after the 30 mm length. Consequently, all the samples used in the determination of its permeability will be 30mm long, and have a diameter of 12,3mm.

According to this, it could be said that the correct length to avoid having entrance effects (in mm) has to be 10 times bigger than the pore size (in µm).

6.2 Parameters obtained

As mentioned before, four different values of the permeability were obtained for each sample, and two for the form coefficient F, based on eq. 14. The method employed to determine each one of them is explained here:

- K_1: permeability of the Forchheimer regime without Darcian velocity correction, which means it has not been divided by the porosity of the foam.

$$K_1 = \frac{\mu_{fluid}}{\frac{\Delta P}{Lv_D}\cdot\left(1+\frac{\Delta P}{2P_0}\right)-\rho_{fluid}\cdot \mathrm{F}\cdot v_D} \qquad (21)$$

- K_2: permeability of the Darcy regime without Darcian velocity correction.

$$K_2 = \left(\frac{\mu_{fluid}}{\frac{\Delta P}{Lv_D}\cdot\left(1+\frac{\Delta P}{2P_0}\right)}\right) \qquad (22)$$

- K_3: permeability of the Forchheimer regime with Darcian velocity correction.

$$K_3 = \frac{\mu_{fluid}}{\frac{\Delta P}{Lv_{DCorr}}\cdot\left(1+\frac{\Delta P}{2P_0}\right)-\rho_{fluid}\cdot \mathrm{F}\cdot v_{DCorr}} \qquad (23)$$

- K_4: permeability of the Darcy regime with Darcian velocity correction.

$$K_4 = \left(\frac{\mu_{fluid}}{\frac{\Delta P}{Lv_{DCorr}}\cdot\left(1+\frac{\Delta P}{2P_0}\right)}\right) \qquad (24)$$

- F1: form coefficient without Darcian velocity correction.

$$F_1 = \frac{\frac{\Delta P}{Lv_D}\cdot\left(1+\frac{\Delta P}{2P_0}\right)}{\rho_{fluid}\cdot v_D} - \frac{\mu_{fluid}}{\mathrm{K}} \qquad (25)$$

- F2: form coefficient with Darcian velocity correction.

$$F_2 = \frac{\frac{\Delta P}{Lv_{DCorr}}\cdot\left(1+\frac{\Delta P}{2P_0}\right)}{\rho_{fluid}\cdot v_{DCorr}} - \frac{\mu_{fluid}}{\mathrm{K}} \qquad (26)$$

The next table shows the results of these 6 parameters obtained for all the samples. The permeability values are expressed in m^2 and the form coefficient values in m^{-1}.

It is noteworthy that all the permeability values, particularly the K_2 permeabilities, are in agreement with the values obtained in [3], in which the permeability of aluminum foams of similar pore size and relative densities made by replication was also measured.

CASTING	Particle Size [µm]	Relative Density	K_1	K_2	K_3	K_4	F_1	F_2
OA	400-450	0,1398	8,37456E-10	7,64876E-10	2,49535E-09	8,89297E-10	8242,491048	11139,45504
OB	400-450	0,1558	7,12648E-10	6,68645E-10	8,44167E-10	7,92043E-10	8740,142058	6228,913928
OC	400-450	0,3042	1,00893E-10	9,64042E-11	1,44996E-10	1,3499E-10	236215,4079	114372,2557
OD	400-450	0,1858	6,18686E-10	5,52001E-10	7,59854E-10	6,77953E-10	19621,92173	13008,35428
OE	180-250	0,3348	-	2,64249E-11	-	3,97259E-11	244357,7579	108119,957
OF	90-125	0,3074	-	1,44244E-11	-	2,08275E-11	188251,2648	90294,15367
OG	180-250	0,1737	2,5351E-10	2,4471E-10	3,06783E-10	2,94932E-10	16175,99923	11045,83703
OH	400-450	0,2711	6,02466E-11	6,05394E-11	8,26525E-11	8,27497E-11	294046,6319	156231,8298
OI	400-450	0,3025	1,47564E-10	1,42183E-10	2,11552E-10	2,00897E-10	166802,2722	81157,83628
OJ	90-125	0,2930	-	4,26823E-11	-	6,03749E-11	19344,63745	9668,15228
OK	400-450	0,2738	2,17086E-10	2,05232E-10	2,98924E-10	2,80265E-10	60554,82269	31936,73836
OL	90-125	0,3970	-	9,85009E-12	-	1,6335E-11	414022,9066	150545,8687
OM	180-250	0,2249	1,36218E-10	1,32501E-10	1,75735E-10	1,7202E-10	24768,85917	14881,82102
ON	90-125	0,3543	-	1,55038E-11	-	2,40108E-11	216618,2186	90314,95795

Table 3: List of the samples measured in this work, detailing its characteristics and the determined values K and F

From these results and from the data analysis process itself, there are some observations to be remarked.

First of all, due to the fact that the Reynolds number has been calculated using the average pore size of the samples (which was assumed to be equal to the salt particle that formed the preforms from which the aluminum foam was infiltrated), there is only three Darcian velocities for the transition from the Darcy to the Forchheimer regime. 425, 215 and 112 µm were chosen as the mean values for each of the particle size ranges, with its corresponding transition Darcian velocity of 0.35, 0.71 and 1.35 $m \cdot s^{-1}$, respectively.

As mentioned before, for the samples with the lower pore size and high relative density the Darcian transition velocity is elevated. This is the reason why the permeability of the Darcy regime (k_2 and k_4) for the OE, OF, OJ, OL and ON castings is the only one that could be determined, because only the Darcy regime was established during the experimentation. It can be asserted that the denser the aluminum foam is, the more flow rate that can be forced into it while holding the Darcy regime.

The fact that these castings are more dense than the others makes it more difficult for the fluid to flow through it, and this combined with the increase of no-slip condition surfaces may provoke that the data plot curve for the permeability determination of these castings does not have the expected shape, so that the validity of these results may be questioned.

The OJ casting data was by far the one whose plotted curve less fitted the expected one. Nonetheless, its permeability parameters for K_2 and K_4 appear to be in agreement with the permeability values for the rest of the 90-125 µm samples, so these values could be credible.

It is also important to emphasize the difference in the parameters determined if the Darcian velocity correction is considered, even more if the aluminum foam has a high density. In fact, the data considered for the K_2 and K_4 permeabilities changes because of this big difference in the velocity, since the velocity of the first one is always lower and so more points are included in the Darcy regime.

At first glance, and considering the permeability range values exposed in the theory (from 10^{-12} to 10^{-6} m^2 for porous metals), the permeability values obtained may be correct. Also, the K_2 values obtained for the OA and OB samples are in accordance with the values obtained in [3] for samples with similar characteristics. Nevertheless, these values will be compared to the model for the permeability by Mortensen [1, 3], to assure its exactness.

Regarding the values obtained for F, it cannot be certain if they are correct. The values for this coefficient in the previous works consulted vary widely according to the source. Considering the given values in [1] for the inertial effects coefficient c_I, which was said to oscillate between 0.03 and 0.11 for metal foams, it can be checked the correctness of the F values obtained. The c_I coefficient for the F_1 and F_2 values obtained in this work will be obtained (eq. 15) and also its corresponding values of the permeability, K_1 and K_3:

CASTING	Particle Size [µm]	Relative Density	K_1	K_3	F_1	F_2	c_{I1}	c_{I2}
OA	400-450	0,1398	8,37E-10	7,20E-10	8242,4	11139,4	0,2385	0,5565
OB	400-450	0,1558	7,13E-10	6,02E-10	8740,1	12263,7	0,2333	0,1810
OC	400-450	0,3042	1,01E-10	7,02E-11	236215,4	487860,6	2,3727	1,3772
OD	400-450	0,1858	6,19E-10	5,04E-10	19621,9	29597,8	0,4881	0,3586
OG	180-250	0,1737	2,54E-10	2,09E-10	16175,9	23688,8	0,2576	0,1935
OH	400-450	0,2711	6,02E-11	4,39E-11	294046,6	553430,2	2,2824	1,4204
OI	400-450	0,3025	1,48E-10	1,03E-10	166802,2	343810,5	2,0262	1,1804
OK	400-450	0,2738	2,17E-10	1,58E-10	60554,82	115321,4	0,8922	0,5522
OM	180-250	0,2249	1,36E-10	1,06E-10	24768,85	42314,4	0,2891	0,1973

Table 4: Form and inertial effects coefficients of the samples

It can be observed that all the c_I coefficients obtained exceed the range of observed values in literature [1], so its validity may be doubted.

However, as the main objective of this work is to determine the permeability of the aluminum foams, and also considering that for high density aluminum foams only the Darcy regime is established, the results of the determination of this parameter will not be given much consideration.

6.3 Comparison to the model

With the objective of verifying and ensuring the validity of permeability values obtained, the permeability of each sample was calculated according to eq. 16. The results of all the permeabilities determined before and the permeability of the model by Mortensen [1, 3], which is specific for metal foams made by replication, are compared in the next table.

CASTING	K_1	K_2	K_3	K_4	K_{model}
OA	8,37456E-10	7,64876E-10	2,49535E-09	8,89297E-10	1,13826E-09
OB	7,12648E-10	6,68645E-10	8,44167E-10	7,92043E-10	9,84628E-09
OC	1,00893E-10	9,64042E-11	1,44996E-10	1,3499E-10	1,16037E-09
OD	6,18686E-10	5,52001E-10	7,59854E-10	6,77953E-10	7,48359E-09
OE	-	2,64249E-11	-	3,97259E-11	8,59769E-11
OF	-	1,44244E-11	-	2,08275E-11	7,3266E-11
OG	2,5351E-10	2,4471E-10	3,06783E-10	2,94932E-10	2,15024E-09
OH	6,02466E-11	6,05394E-11	8,26525E-11	8,27497E-11	2,44269E-09
OI	1,47564E-10	1,42183E-10	2,11552E-10	2,00897E-10	1,21664E-09
OJ	-	4,26823E-11	-	6,03749E-11	1,07511E-10
OK	2,17086E-10	2,05232E-10	2,98924E-10	2,80265E-10	2,32407E-09
OL	-	9,85009E-12	-	1,6335E-11	-
OM	1,36218E-10	1,32501E-10	1,75735E-10	1,7202E-10	1,24548E-09
ON	-	1,55038E-11	-	2,40108E-11	2,44062E-12

Table 5: Comparison between the theoretical values of the permeability for the metal foams made by replication and the values obtained in this work

The value of the model permeability the sample OL could not be obtained. This is because the relative density of this foam is so high (above 0.36, the V_o value employed), that the second term of eq. 16 becomes the square root of a negative number.

Even though the permeability values obtained experimentally and the ones predicted by the model differ up to an order of magnitude, the conclusion of which of the four determined permeabilities is more close to the value assumed as correct can still be extracted. The difference between the values predicted by the model may be a consequence of the fact that maybe the value of the volume fraction of the preform before densification of 0.64 used in this calculation is not valid for the salt preforms made in this work, because the salt particles are not spherical enough. To try to amend this possible error, information about the preforms (i.e. the relation between weight of the salt and the volume of the rubber cylinder where it has been introduced) could be used as a reference for the level of compacting before densification, instead of the 0.64 value. Another possible explanation is that this model was developed in [3] for aluminum foams made by the replication method and with relative densities from 12% to 32% (as has also been done in this work), but using a liquid (water or glycerine) as a fluid flowing through the aluminum foam. It may be possible that this model is not suitable if the fluid employed is a gas, which have different properties and behaviour than liquid fluids (e.g. compressibility effects, establishment of the Forchheimer regime).

By comparing the total error between the four permeabilities and the one calculated by the model, it can be concluded that the permeabilities that account for the Darcian velocity correction tend to be more close to the model value. Furthermore, the permeability values that only consider the Darcy regime are more accurate that the ones obtained by considering all the data that is related to the Forchheimer regime. Accordingly, the permeabilities ordered by its accuracy in fitting the model are K_4, K_2, K_3 and K_1. This is due to the fact that the model is based in the Darcy regime definition of permeability.

6.4 Correlations and dependencies

It was indicated at the introduction that the primary objective of this work was to deduce a correlation between the aluminum foam characteristics (the pore size and the relative density) and its permeability.

By examining the plotted curves for each sample is clear that the castings OL, ON and OF are the ones offering more resistance to the flow passing through them, as their permeabilities are lower. This is due to the fact that their curve crosses the vertical axis at high values, and the permeability of a foam is inversely proportional to the intersection with the vertical axis. These three foams, along with the OJ castings, are the ones with the smaller pore size (from 90 to 125 µm), so it is evident that the permeability of the aluminum foam is a direct consequence of its pore size. It has to be considered as well that all the samples with pore size of 90-125 µm are very dense, with relative densities from 29% to 39%. Hence, it cannot be affirmed yet which of this parameters is more influential for the permeability. With the aim of differentiating the possible effects of both the pore size and the relative density of the aluminum in its permeability, they will be plotted separately.

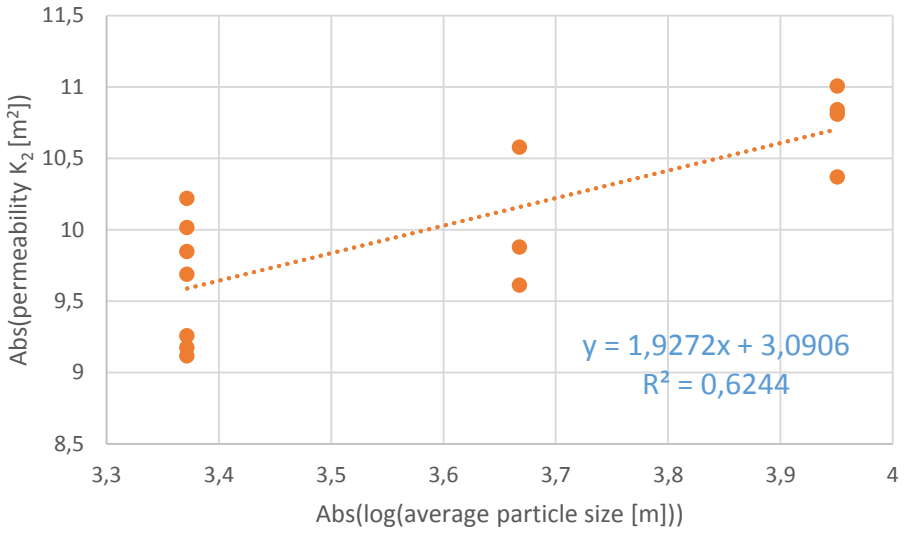

Figure 22: K_2 permeability values obtained for each particle size and its tendency line

By contemplating *figure 22,* it can be straightforwardly accepted that the pore size has a strong effect on the permeability, and it seems that the permeability may be proportional to the average pore squared. Moreover, the average pore size also appears to determine the range of permeability values that a sample can reach; so the lower the pore size the lower the maximum value of permeability that the aluminum foam can have. Nonetheless, as may be noticed if the permeability values of the 400-450 µm samples are analysed, the permeability value is also intensely dependent on the relative density of the foam. Is this relative density the parameter that provokes such disparity within the 400-450 µm samples, whose relative densities vary from 14% to 30%. This effect can also be perceived, at lesser extent, for the 180-250 µm samples, which relative densities go from 22% to 33%.

On the other hand, if the uncorrected Darcian permeability (K_2) values are plotted together regarding the relative density of the foams, as has been done in *figure 23*, it can be readily seen that the permeability is directly linked to the metal foam relative density. However, as it has been confirmed in the past analysis, the pore size is also affecting the permeability values, as can be checked by the low values of permeability obtained for low relative density foams.

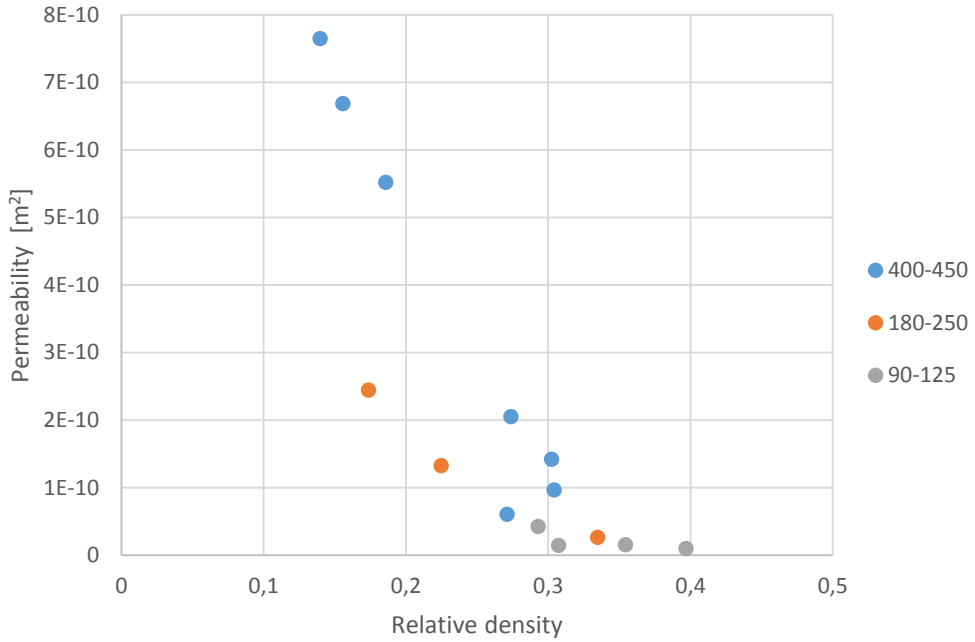

Figure 23: K_2 permeability values obtained for the different relative densities of the foams and pore size

For a better understanding the possible interaction of the two parameters in the permeability of the aluminum foams, the K_2 value of the permeability has been plotted for each pore size and relative density *(figure 24)*. The K_2 value has been chosen because of its agreement with previous experimental data and also since there are permeability values of all the castings. The negative logarithm of the K_2 value has been plotted in order to facilitate the distinction of the individual permeability values, which vary from each other in one or two orders of magnitude, being difficult to compare otherwise, and the same has been done to the values of the relative densities.

After reviewing this last graph, it can be concluded that both the pore size and the relative density of the foam have a decisive effect on the aluminum foam permeability. Such conclusion can be proved easily by the 400-450 µm foams with approximately 30% relative densities, whose permeability is as low as the one of the 180-250 µm and 20% relative density. Likewise, for samples with the same pore size the permeability varies extensively depending on its relative density, as may be perceived for all the 400-450 µm samples. Nonetheless, for the same relative density the permeability also differs greatly depending on the pore size of the foam, as may be demonstrated by the 400-450, 180-250 and 90-125 µm samples with nearly 30% relative density each.

It must be remarked that, even though they have the same pore size and very similar relative densities, the OH and OK castings permeability differ more than expected, regarding the similarity of their parameters. This may be due to the possible experimentation error, or to the fact that, when inserting the sample OH in its container, more force than usual had to be applied. This was because the diameter of this sample was too big to perfectly fit its container, and possibly when forcing the foam into the container the front face of it may have been deformed, closing the pores and so hampering the fluid flow. This last reason may explain why OH casting permeability is almost ten times lower than that of the OK casting. The same may also have occurred with samples of the castings OC and OI, the latter having lower permeability because it was tried to be inserted into the container unsuccessfully before covering it with the white and thinner thermo shrinkable plastic.

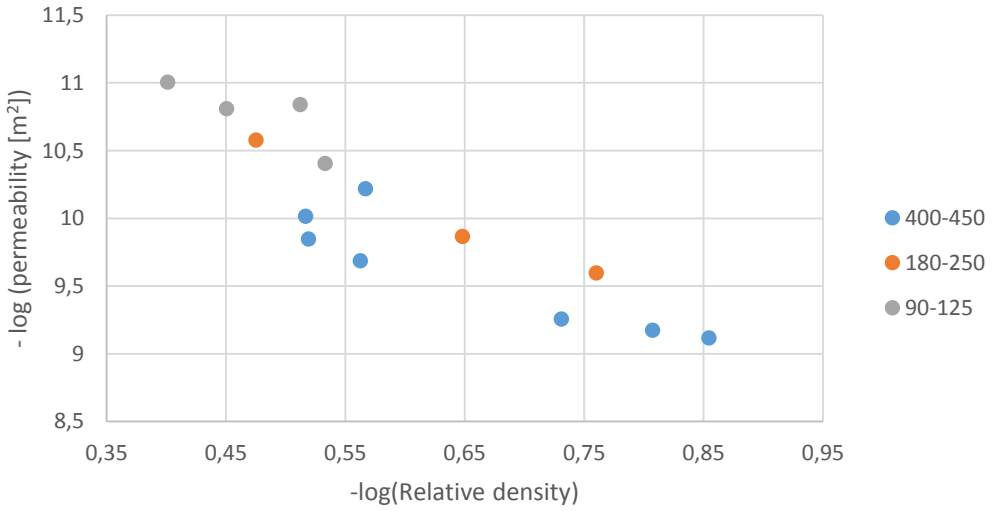

Figure 24: - log (K_2) values for each pore size and relative density

Lastly, it is necessary to highlight the case of the OL casting, that combines both high relative density and small pore size, and this makes its permeability drop dramatically.

7 FUTURE WORK

Once that the strong dependency of the characteristics and properties of the aluminum foam on the parameters that define its internal pore structure has been proved, the next step would be deducting a correlation of these parameters and the final characteristics of the aluminum foam, as the permeability or its form coefficient. This way, the foam with the exact properties desired could be made by choosing its pore size and relative density.

But even if this correlation is known, it will still be necessary to find a more precise prediction of the relative density of the preform that will be obtained depending on the CIP pressure applied, so as to be able to fabricate the desired preform. The effects of the infiltration pressure on the resulting aluminum foam has been noticed by this work, so a study could be made to investigate this dependency more deeply.

Finally, it would be also recommendable to proceed with this experimentation as it was done in this work, but this time applying a different outlet pressure. If the pressure at the end of the container of the sample is not the atmospheric pressure, the foam will be subjected to higher pressures, and its behaviour under this conditions could be studied. The air flowing through it will have even more compressibility effect, and the increase of the differential pressure between the ends of the container will create a different fluid flow than the one that has been experienced in this work. It would be also interesting, though, to perform this same experiment with other gases, such as helium or argon, in order to determine how the gas properties affect the fluid flowing phenomena through porous medium.

8 CONCLUSIONS

The values of the permeability as well as the form coefficient has been determined for a set of different aluminum foams. These foams were produced in the laboratory with the intention that they had some specific characteristics that will determine their final properties.

Initially, the preforms had to be made so that the aluminum foams could be obtained by infiltration. The salt particle size chosen to form the preform as well as the applied pressure at the CIP process regulate its final relative density, and so the porosity of the future aluminum foam that will be created from this preform. The relationship between the particle size, the desired porosity of the preform and the corresponding CIP pressure that has to be applied is not yet well precise enough, so the resulting preforms do not have the expected porosity. This relationship could be analysed in order to expedite the process of manufacturing the preforms.

Moreover, the porosity of the preform will determine the posterior relative density of the aluminum foam, as they are both values almost the same. That means that if the preform has a porosity of 20%, the aluminum foam relative density will be nearly 20%. The values are not identical because some air or salt particles may remain inside the aluminum foam, or even some salt from the preform may be detached during the infiltration, as the liquid aluminum fills the air gaps that conform the pores of the preform. This fact also clarifies the strong correlation between the relative density of the foam and its permeability, because the flowing fluid will be able to flow through the porous structure, which was earlier the salt preform structure. It is affirmed that the permeability of the aluminum foam increases with its porosity.

However, the parameter that has also proven to be relevant in the permeability value of the aluminum foam is the pore size, which turns out to be the salt particle size that was used for the preform. If the salt particle is big enough, the contact area between them while forming the preform will also be large. Once the infiltration is done, this area will form a “window” between the pores, and the ensemble of windows will form a path through which the air can flow, increasing the permeability of the foam. Nonetheless, if the salt particle is small, these contacts make not take place, closing the possible routes for the flow, and thus decreasing radically the permeability. It is demonstrated, therefore, that the bigger the pore size the more permeable the aluminum foam will be.

On the other hand, the measurements of the aluminum foams with high densities gave poor results that hardly did not fit the expected curve for the phenomena. This detail may be a consequence of the importance of taking into account the no-slip condition, that hiders the establishment of a steady flow inside the foam.

In this work has been initially considered the Darcy-Forchheimer equation to describe the fluid flow phenomena through a porous medium. Notwithstanding, as has been experienced

with the aluminum foams, especially for the ones with small pore size and high density, normally only the Darcy regime was established. This is due in part to the fact that the limitation of the pressure gauge would not permit increasing the volumetric flow rate inside the foam, so the maximum speed was restricted. This experiment could be done with higher flow velocities if the pressure gauge was upgraded. By having more measurements of flow in the Forchheimer regime, the inertia of the flow and the drag caused by the microstructure of the aluminum foam could be analysed.

Lastly, regarding the correction of the permeability values obtained by this experiments, it is necessary to point that their validity may only be verified by comparison with the existing works on the subject or with the models already developed for it. This is what has been done with the values obtained in this work, which are in the range of the values expected for aluminum foams and obtained in previous studies, but diverge widely with the values predicted using the model. It would be necessary now to analyse if there are some factors which may have caused this difference or if the model is not appropriate for the fluid employed in this work.

Whatever the case, the results of this study can help understanding the parameters that affect the fluid flow through porous medium, and more specifically, it may serve as a guide to manufacture samples similar to the ones used in this work.

ACKNOWLEGMENTS

I would like to thank my tutor of this work, professor Dr. Ludger Weber for his assistance and attention during this project. I would also like to thank Alex Athanasiou-Ioannou for his help, and for being always there to lend me the keys of the laboratories, without forgetting the pleasant people at the laboratories that have done my work easier. I would not have been able to fulfil this project without all this help.

9 REFERENCES

[1] Russell Goodall and Andreas Mortensen*, Chapter 26: Porous metals*, PHYSICAL METALLURGY – fifth edition, Editors *David Lauhlin and Kazuhiro Hono*, Elsevier, Amsterdam.

[2] Dr. R. W. Zimmerman, *Flow in Porous Media,* book for the M.Sc. in Petroleum Engineering 2003-2004, Department of Earth Science and Engineering, Imperial College London.

[3] Jean-François Despois and Andreas Mortensen, *Permeability of open-pore microcellular materials,* A. 2005, Acta Materialia 53 (2005) 1381–1388.

[4] Nihad Dukhan, *Analysis of Brinkman-Extended Darcy flow in porous media and experimental verification using metal foam*, ASME, Journals of Fluids Engineering, July 2012, Vol. 143, 071201-1.

[5] Nihad Dukhan and Mohamed Ali, *Strong wall and transverse size effects of pressure drop of flow through open-cell metal foam*, Department of Mechanical Engineering of the University of Detroit, Elsevier Mason SAS., International journal of Thermal Sciences 57 (2012) 85-91.

[6] M .D M. Innocentini, L. P. Lefebre, R. V. Meloni and E. Baril, *Influence of sample thickness and measurement set-up on the experimental evaluation of permeability of metallic foams,* Springer 2009.

[7] Louis-Philippe Lefebvre, John Banhart and David C. Dunand, *Porous Metals and Metallic Foams: Current Status and Recent Developments,* ADVANCED ENGINEERING MATERIALS 2008, 10, No. 9.

[8] Nihad Dukhan and Krunal Patel*, Effect of sample's length on flow properties of open-cell metal foam and pressure-drop correlations*, J Porous Mater (2011) 18:655–665.

[9] Jean-Philippe Bonnet,Frederic Topin and Lounes Tadrist, *Flow Laws in Metal Foams: Compressibility and Pore Size Effects,* Transp Porous Med (2008) 73:233–254.

[10] Nihad Dukhan and Mohamed Ali*, Effect of confining wall on properties of gas flow through metal foam: an experimental study*, Transp Porous Med (2012) 91:225–237.

[11] Nihad Dukhan and Carel A. Minjeur, *A two-permeability approach for assessing flow properties in metal foam*, J Porous Mater (2011) 18:417–424.

[12] Nihad Dukhan, *Metal foams: fundamentals and applications*, 2013 DESTech publications.

[13] Yu-Shu Wu, Karsten Pruess and Peter Persoff, *Glas flow in Porous media with Kinkenberg effects*, 1998, 117-137.

[14] Mamoun Medraj, Edric Baril, Virendra Loya and Louis-Philippe Lefebvre, *The effect of microstructure on the permeability of metallic foams*, 2007, 42; 4371-4383.

[15] Maria Cecilia Bravo, *Effect of transition from slip to free molecular flow on gas transport in porous media*, 10.1063/1.2786613.